

This is the accepted manuscript made available via CHORUS, the article has been published as:

Observation of Two New N^{\ast} Resonances in the Decay $\psi(3686) \rightarrow p\bar{p}[\overline{}]\pi^0$

M. Ablikim *et al.* (BESIII Collaboration)

Phys. Rev. Lett. **110**, 022001 — Published 11 January 2013

DOI: [10.1103/PhysRevLett.110.022001](https://doi.org/10.1103/PhysRevLett.110.022001)

Observation of two new N^* resonances in $\psi(3686) \rightarrow p\bar{p}\pi^0$

M. Ablikim¹, M. N. Achasov⁵, D. J. Ambrose⁴⁰, F. F. An¹, Q. An⁴¹, Z. H. An¹, J. Z. Bai¹, Y. Ban²⁷, J. Becker², N. Berger¹, M. Bertani¹⁸, J. M. Bian³⁹, E. Boger^{20,a}, O. Bondarenko²¹, I. Boyko²⁰, R. A. Briere³, V. Bytev²⁰, X. Cai¹, A. Calcaterra¹⁸, G. F. Cao¹, J. F. Chang¹, G. Chelkov^{20,a}, G. Chen¹, H. S. Chen¹, J. C. Chen¹, M. L. Chen¹, S. J. Chen²⁵, Y. Chen¹, Y. B. Chen¹, H. P. Cheng¹⁴, Y. P. Chu¹, D. Cronin-Hennessy³⁹, H. L. Dai¹, J. P. Dai¹, D. Dedovich²⁰, Z. Y. Deng¹, A. Denig¹⁹, I. Denysenko^{20,b}, M. Destefanis⁴⁴, W. M. Ding²⁹, Y. Ding²³, L. Y. Dong¹, M. Y. Dong¹, S. X. Du⁴⁷, J. Fang¹, S. S. Fang¹, L. Fava^{44,c}, F. Feldbauer², C. Q. Feng⁴¹, R. B. Ferrol¹⁸, C. D. Fu¹, J. L. Fu²⁵, Y. Gao³⁶, C. Geng⁴¹, K. Goetzen⁷, W. X. Gong¹, W. Gradl¹⁹, M. Greco⁴⁴, M. H. Gu¹, Y. T. Gu⁹, Y. H. Guan⁶, A. Q. Guo²⁶, L. B. Guo²⁴, Y. P. Guo²⁶, Y. L. Han¹, X. Q. Hao¹, F. A. Harris³⁸, K. L. He¹, M. He¹, Z. Y. He²⁶, T. Held², Y. K. Heng¹, Z. L. Hou¹, H. M. Hu¹, J. F. Hu⁶, T. Hu¹, B. Huang¹, G. M. Huang¹⁵, J. S. Huang¹², X. T. Huang²⁹, Y. P. Huang³⁶, T. Hussain⁴³, C. S. Ji⁴¹, Q. Ji¹, X. B. Ji¹, X. L. Ji¹, L. K. Jia¹, L. L. Jiang¹, X. S. Jiang¹, J. B. Jiao²⁹, Z. Jiao¹⁴, D. P. Jin¹, S. Jin¹, F. F. Jing³⁶, N. Kalantar-Nayestanaki²¹, M. Kavatsyuk²¹, W. Kühn³⁷, W. Lai¹, J. S. Lange³⁷, J. K. C. Leung³⁵, C. H. Li¹, Cheng Li⁴¹, Cui Li⁴¹, D. M. Li⁴⁷, F. Li¹, G. Li¹, H. B. Li¹, J. C. Li¹, K. Li¹⁰, Lei Li¹, N. B. Li²⁴, Q. J. Li¹, S. L. Li¹, W. D. Li¹, W. G. Li¹, X. L. Li²⁹, X. N. Li¹, X. Q. Li²⁶, X. R. Li²⁸, Z. B. Li³³, H. Liang⁴¹, Y. F. Liang³¹, Y. T. Liang³⁷, G. R. Liao³⁶, X. T. Liao¹, B. J. Liu³⁴, B. J. Liu¹, C. L. Liu³, C. X. Liu¹, C. Y. Liu¹, F. H. Liu³⁰, Fang Liu¹, Feng Liu¹⁵, H. Liu¹, H. B. Liu⁶, H. H. Liu¹³, H. M. Liu¹, H. W. Liu¹, J. P. Liu⁴⁵, K. Y. Liu²³, Kai Liu⁶, Kun Liu²⁷, P. L. Liu²⁹, S. B. Liu⁴¹, X. Liu²², X. H. Liu¹, Y. Liu¹, Y. B. Liu²⁶, Z. A. Liu¹, Zhiqiang Liu¹, Zhiqing Liu¹, H. Loehner²¹, G. R. Lu¹², H. J. Lu¹⁴, J. G. Lu¹, Q. W. Lu³⁰, X. R. Lu⁶, Y. P. Lu¹, C. L. Luo²⁴, M. X. Luo⁴⁶, T. Luo³⁸, X. L. Luo¹, M. Lv¹, C. L. Ma⁶, F. C. Ma²³, H. L. Ma¹, Q. M. Ma¹, S. Ma¹, T. Ma¹, X. Y. Ma¹, Y. Ma¹¹, F. E. Maas¹¹, M. Maggiora⁴⁴, Q. A. Malik⁴³, H. Mao¹, Y. J. Mao²⁷, Z. P. Mao¹, J. G. Messchendorp²¹, J. Min¹, T. J. Min¹, R. E. Mitchell¹⁷, X. H. Mo¹, C. Morales Morales¹¹, C. Motzko², N. Yu. Muchnoi⁵, Y. Nefedov²⁰, C. Nicholson⁶, I. B. Nikolaev⁵, Z. Ning¹, S. L. Olsen²⁸, Q. Ouyang¹, S. Pacetti^{18,d}, J. W. Park²⁸, M. Pelizaeus³⁸, K. Peters⁷, J. L. Ping²⁴, R. G. Ping¹, R. Poling³⁹, E. Prencipe¹⁹, C. S. J. Pun³⁵, M. Qi²⁵, S. Qian¹, C. F. Qiao⁶, X. S. Qin¹, Y. Qin²⁷, Z. H. Qin¹, J. F. Qiu¹, K. H. Rashid⁴³, G. Rong¹, X. D. Ruan⁹, A. Sarantsev^{20,e}, J. Schulze², M. Shao⁴¹, C. P. Shen^{38,f}, X. Y. Shen¹, H. Y. Sheng¹, M. R. Shepherd¹⁷, X. Y. Song¹, S. Spataro⁴⁴, B. Spruck³⁷, D. H. Sun¹, G. X. Sun¹, J. F. Sun¹², S. S. Sun¹, X. D. Sun¹, Y. J. Sun⁴¹, Y. Z. Sun¹, Z. J. Sun¹, Z. T. Sun⁴¹, C. J. Tang³¹, X. Tang¹, E. H. Thorndike⁴⁰, H. L. Tian¹, D. Toth³⁹, M. Ullrich³⁷, G. S. Varner³⁸, B. Wang⁹, B. Q. Wang²⁷, J. X. Wang¹, K. Wang¹, L. L. Wang⁴, L. S. Wang¹, M. Wang²⁹, P. Wang¹, P. L. Wang¹, Q. Wang¹, Q. J. Wang¹, S. G. Wang²⁷, X. F. Wang¹², X. L. Wang⁴¹, Y. D. Wang⁴¹, Y. F. Wang¹, Y. Q. Wang²⁹, Z. Wang¹, Z. G. Wang¹, Z. Y. Wang¹, D. H. Wei⁸, P. Weidenkaff¹⁹, Q. G. Wen⁴¹, S. P. Wen¹, M. Werner³⁷, U. Wiedner², L. H. Wu¹, N. Wu¹, S. X. Wu⁴¹, W. Wu²⁶, Z. Wu¹, L. G. Xia³⁶, Z. J. Xiao²⁴, Y. G. Xie¹, Q. L. Xiu¹, G. F. Xu¹, G. M. Xu²⁷, H. Xu¹, Q. J. Xu¹⁰, X. P. Xu³², Y. Xu²⁶, Z. R. Xu⁴¹, F. Xue¹⁵, Z. Xue¹, L. Yan⁴¹, W. B. Yan⁴¹, Y. H. Yan¹⁶, H. X. Yang¹, T. Yang⁹, Y. Yang¹⁵, Y. X. Yang⁸, H. Ye¹, M. Ye¹, M. H. Ye⁴, B. X. Yu¹, C. X. Yu²⁶, J. S. Yu²², S. P. Yu²⁹, C. Z. Yuan¹, W. L. Yuan²⁴, Y. Yuan¹, A. A. Zafar⁴³, A. Zallo¹⁸, Y. Zeng¹⁶, B. X. Zhang¹, B. Y. Zhang¹, C. C. Zhang¹, D. H. Zhang¹, H. H. Zhang³³, H. Y. Zhang¹, J. Zhang²⁴, J. G. Zhang¹², J. Q. Zhang¹, J. W. Zhang¹, J. Y. Zhang¹, J. Z. Zhang¹, L. Zhang²⁵, S. H. Zhang¹, T. R. Zhang²⁴, X. J. Zhang¹, X. Y. Zhang²⁹, Y. Zhang¹, Y. H. Zhang¹, Y. S. Zhang⁹, Z. P. Zhang⁴¹, Z. Y. Zhang⁴⁵, G. Zhao¹, H. S. Zhao¹, J. W. Zhao¹, K. X. Zhao²⁴, Lei Zhao⁴¹, Ling Zhao¹, M. G. Zhao²⁶, Q. Zhao¹, S. J. Zhao⁴⁷, T. C. Zhao¹, X. H. Zhao²⁵, Y. B. Zhao¹, Z. G. Zhao⁴¹, A. Zhemchugov^{20,a}, B. Zheng⁴², J. P. Zheng¹, Y. H. Zheng⁶, Z. P. Zheng¹, B. Zhong¹, J. Zhong², L. Zhou¹, X. K. Zhou⁶, X. R. Zhou⁴¹, C. Zhu¹, K. Zhu¹, K. J. Zhu¹, S. H. Zhu¹, X. L. Zhu³⁶, X. W. Zhu¹, Y. M. Zhu²⁶, Y. S. Zhu¹, Z. A. Zhu¹, J. Zhuang¹, B. S. Zou¹, J. H. Zou¹, J. X. Zuo¹

(BESIII Collaboration)

¹ Institute of High Energy Physics, Beijing 100049, P. R. China

² Bochum Ruhr-University, 44780 Bochum, Germany

³ Carnegie Mellon University, Pittsburgh, PA 15213, USA

⁴ China Center of Advanced Science and Technology, Beijing 100190, P. R. China

⁵ G.I. Budker Institute of Nuclear Physics SB RAS (BINP), Novosibirsk 630090, Russia

⁶ Graduate University of Chinese Academy of Sciences, Beijing 100049, P. R. China

⁷ GSI Helmholtzcentre for Heavy Ion Research GmbH, D-64291 Darmstadt, Germany

⁸ Guangxi Normal University, Guilin 541004, P. R. China

⁹ Guangxi University, Nanning 530004, P. R. China

¹⁰ Hangzhou Normal University, Hangzhou 310036, P. R. China

¹¹ Helmholtz Institute Mainz, J.J. Becherweg 45, D 55099 Mainz, Germany

¹² Henan Normal University, Xinxiang 453007, P. R. China

¹³ Henan University of Science and Technology, Luoyang 471003, P. R. China

¹⁴ Huangshan College, Huangshan 245000, P. R. China

¹⁵ Huazhong Normal University, Wuhan 430079, P. R. China

¹⁶ Hunan University, Changsha 410082, P. R. China

¹⁷ Indiana University, Bloomington, Indiana 47405, USA

¹⁸ INFN Laboratori Nazionali di Frascati, Frascati, Italy

¹⁹ Johannes Gutenberg University of Mainz, Johann-Joachim-Becher-Weg 45, 55099 Mainz, Germany

²⁰ Joint Institute for Nuclear Research, 141980 Dubna, Russia

²¹ KVI/University of Groningen, 9747 AA Groningen, The Netherlands

- ²² Lanzhou University, Lanzhou 730000, P. R. China
²³ Liaoning University, Shenyang 110036, P. R. China
²⁴ Nanjing Normal University, Nanjing 210046, P. R. China
²⁵ Nanjing University, Nanjing 210093, P. R. China
²⁶ Nankai University, Tianjin 300071, P. R. China
²⁷ Peking University, Beijing 100871, P. R. China
²⁸ Seoul National University, Seoul, 151-747 Korea
²⁹ Shandong University, Jinan 250100, P. R. China
³⁰ Shanxi University, Taiyuan 030006, P. R. China
³¹ Sichuan University, Chengdu 610064, P. R. China
³² Soochow University, Suzhou 215006, China
³³ Sun Yat-Sen University, Guangzhou 510275, P. R. China
³⁴ The Chinese University of Hong Kong, Shatin, N.T., Hong Kong.
³⁵ The University of Hong Kong, Pokfulam, Hong Kong
³⁶ Tsinghua University, Beijing 100084, P. R. China
³⁷ Universität Giessen, 35392 Giessen, Germany
³⁸ University of Hawaii, Honolulu, Hawaii 96822, USA
³⁹ University of Minnesota, Minneapolis, MN 55455, USA
⁴⁰ University of Rochester, Rochester, New York 14627, USA
⁴¹ University of Science and Technology of China, Hefei 230026, P. R. China
⁴² University of South China, Hengyang 421001, P. R. China
⁴³ University of the Punjab, Lahore-54590, Pakistan
⁴⁴ University of Turin and INFN, Turin, Italy
⁴⁵ Wuhan University, Wuhan 430072, P. R. China
⁴⁶ Zhejiang University, Hangzhou 310027, P. R. China
⁴⁷ Zhengzhou University, Zhengzhou 450001, P. R. China

^a also at the Moscow Institute of Physics and Technology, Moscow, Russia

^b on leave from the Bogolyubov Institute for Theoretical Physics, Kiev, Ukraine

^c University of Piemonte Orientale and INFN (Turin)

^d Currently at INFN and University of Perugia, I-06100 Perugia, Italy

^e also at the PNPI, Gatchina, Russia

^f now at Nagoya University, Nagoya, Japan

(Dated: November 26, 2012)

Based on $106 \times 10^6 \psi(3686)$ events collected with the BESIII detector at the BEPCII facility, a partial wave analysis of $\psi(3686) \rightarrow p\bar{p}\pi^0$ is performed. The branching fraction of this channel has been determined to be $B(\psi(3686) \rightarrow p\bar{p}\pi^0) = (1.65 \pm 0.03 \pm 0.15) \times 10^{-4}$. In this decay, 7 N^* intermediate resonances are observed. Among these, two new resonances, $N(2300)$ and $N(2570)$ are significant, one $1/2^+$ resonance with a mass of $2300^{+40+109}_{-30-0}$ MeV/ c^2 and width of $340^{+30+110}_{-30+58}$ MeV/ c^2 , and one $5/2^-$ resonance with a mass of 2570^{+19+34}_{-10-10} MeV/ c^2 and width of 250^{+14+69}_{-24-21} MeV/ c^2 . For the remaining 5 N^* intermediate resonances ($N(1440)$, $N(1520)$, $N(1535)$, $N(1650)$ and $N(1720)$), the analysis yields mass and width values which are consistent with those from established resonances.

PACS numbers: 14.20.Gk, 14.40.Lb, 11.80.Et

Although symmetric non-relativistic three-quark models of baryons are quite successful in interpreting low-lying excited baryon resonances, they tend to predict far more excited states than are found experimentally (“missing resonance problem”) [1, 2]. From the theoretical point of view, this could be due to a wrong choice of the degrees of freedom, and models considering di-quarks have been proposed [3]. Experimentally, the situation is very complicated due to the large number of broad and overlapping states that are observed. Moreover, in traditional studies using tagged photons or pion beams [4–11], both isospin 1/2 and isospin 3/2 resonances are excited, further complicating the analysis.

An alternative method to investigate nucleon

resonances employs decays of charmonium states such as J/ψ and $\psi(3686)$. By selecting specific decay channels, such as $\psi(3686) \rightarrow p\bar{p}\pi^0$, N^* intermediate resonances coupling to $p\pi^0$ or $\bar{p}\pi^0$ can be studied. Here, Δ resonances are suppressed due to isospin conservation. As a consequence, the reduced number of states greatly facilitates the analysis [12].

N^* production in $J/\psi \rightarrow p\bar{p}\eta$ was studied using partial wave analysis at BES [13], and two N^* resonances were observed. In a recent analysis of $J/\psi \rightarrow p\bar{n}\pi^- + c.c.$ [14], a new N^* resonance around 2000 MeV/ c^2 named $N(2065)$ was observed. This $N(2065)$ was also observed in the decay of $J/\psi \rightarrow p\bar{p}\pi^0$ [15]. The production of $N(2065)$ in J/ψ decays occurs close to the edge of the phase space. Thus, a similar search for this resonance in the $\psi(3686)$

decays should provide further insight.

In the work of the CLEO Collaboration [16], $\psi(3686) \rightarrow p\bar{p}\pi^0$ was studied using $24.5 \times 10^6 \psi(3686)$ events. With the invariant mass spectra of $p\pi^0$ and $p\bar{p}$, two N^* resonances ($N(1440)$, $N(2300)$) and two $p\bar{p}$ resonances ($R_1(2100)$, $R_2(2900)$) were investigated without taking into account possible interferences between the resonances. The inclusion of $R(2100)$ is suggested by a threshold enhancement in the $p\bar{p}$ mass spectrum. The concentration of events below 1800 MeV/ c^2 in the $p\pi^0$ mass spectrum is considered as the contribution of $N(1440)$ alone.

In this Letter, we briefly report a study of N^* resonances from $\psi(3686) \rightarrow p\bar{p}\pi^0$ based on a data sample of 160 pb^{-1} corresponding to 106 million $\psi(3686)$ decays collected with the upgraded Beijing Spectrometer (BESIII), located at the Beijing Electron-Positron Collider (BEPCII) [17]. The full details will be published later.

The BESIII detector is composed of a helium-gas based drift chamber (MDC), a time-of-flight (TOF) system, a CsI (TI) electromagnetic calorimeter (EMC), a super-conducting solenoid magnet and a resistive plate chambers based muon chamber. More detailed information about the detector can be found in Ref. [17].

The final state in this decay is characterized by two charged tracks and two photons. Two charged tracks with opposite charge are required. Each track is required to have its point of closest approach to the beam axis within ± 20 cm of the interaction point in the beam direction and within 2 cm of the beam axis in the plane perpendicular to the beam. The polar angle of the track is required to be within the region of $|\cos(\theta)| < 0.8$.

The TOF and the specific energy loss dE/dx of a particle measured in the MDC are combined to calculate particle identification (PID) probabilities for pion, kaon and proton hypotheses. For each track, the particle type yielding the largest probability is assigned. In this analysis, one charged track is required to be identified as a proton and the other one as an anti-proton.

Photon candidates are selected by requiring a minimum energy deposition of 25 MeV in the barrel EMC or 50 MeV in the endcap EMC. To reject photons due to charged particle radiation production, the angle between the photon candidate and the proton is required to be greater than 10° . A more stringent cut of 30° between the photon candidate and anti-proton is applied to exclude the large number of photons from anti-proton annihilation.

For events with one proton, one anti-proton and at least two photons, a kinematic fit (4C) with the sum of four-momenta of all particles constrained to the energy and three momentum-components of the initial e^+e^- system is applied. A further kinematic fit (5C) with one more constraint of π^0 mass for the two photons is applied to provide more accurate momentum information of the

final states. When more than two photons are found in a candidate event, all possible $p\bar{p}\gamma\gamma$ combinations are considered and the one yielding the smallest χ^2_{5C} is retained for further analysis.

The events passing the above selection criteria are shown in plots (a) and (b) of Fig. 1, displayed as the Dalitz plot of $\psi(3686) \rightarrow p\bar{p}\pi^0$ and the invariant mass of $p\bar{p}$. The $p\bar{p}$ mass spectrum shows a clear J/ψ signal. Due to the detector resolution, the observed width of J/ψ is far larger than its natural width. This width difference causes a problem in the inclusion of J/ψ in partial wave analysis. Thus, a cut of $|M_{p\bar{p}} - M_{J/\psi}| > 40 \text{ MeV}/c^2$ is applied to exclude events with $p\bar{p}$ arising from J/ψ decay. 4988 events survive the event selection criteria. The mass spectra of $p\pi^0$ and $\bar{p}\pi^0$ for the surviving events are shown in Fig. 1 (c) and (d).

For this analysis, two background sources are studied. The first one arises from $\psi(3686)$ decays and has been studied with two methods. In the first method, a sample of 10^8 Monte Carlo (MC)-simulated $\psi(3686)$ events is used and forty events survive the event selection, mainly due to misidentified or lost photons. In the second method, the background contribution is estimated using the π^0 sideband events, defined by $30 \text{ MeV}/c^2 < |M_{\gamma\gamma} - 135| < 45 \text{ MeV}/c^2$. Only 26 events are found in the sideband area. The other background source arises from the continuum process $e^+e^- \rightarrow \gamma^* \rightarrow p\bar{p}\pi^0$. This has been studied using 42 pb^{-1} of continuum data at $\sqrt{s} = 3650 \text{ MeV}$. After normalizing to the integrated luminosity of $\psi(3686)$, 447 background events are found. In Fig. 1, the shaded histograms show the total background contributions from continuum process and π^0 sideband, in which the continuum contribution accounts for about 95%.

In our present investigation, with larger statistics than at CLEOc, more than one N^* state below 1700 MeV/ c^2 is seen in the $p\pi^0$ and $\bar{p}\pi^0$ mass spectra, and the threshold enhancement in the $p\bar{p}$ mass spectrum is also visible. To better understand the components of this decay, a partial wave analysis taking into account the possible interferences is pursued.

The decay of $\psi(3686) \rightarrow p\bar{p}\pi^0$ is thought to be dominated by two-body decays involving N^* , \bar{N}^* states [18], which can be described by $\psi(3686) \rightarrow p\bar{N}^*(\bar{p}N^*)$, $N^*(\bar{N}^*) \rightarrow p\pi^0(\bar{p}\pi^0)$. In addition, a process of the type $\psi(3686) \rightarrow R\pi^0$ is considered, where R represents a hypothetical $p\bar{p}$ resonance. The data are fitted applying an unbinned maximum likelihood fit. The amplitudes (A_i) for all possible partial waves are constructed using the relativistic covariant tensor amplitude formalism [15, 19, 20]. With these amplitudes, the total transition probability for each event is obtained from a linear combination of these partial wave amplitudes as $\omega = |\sum_i c_i A_i|^2$. Finally the likelihood function $\ln(L)$ is constructed as $\sum_{i=1}^n \ln(\frac{\omega(\xi_i)\epsilon(\xi_i)}{\int d\xi \omega(\xi_i)\epsilon(\xi_i)})$, where n is the total

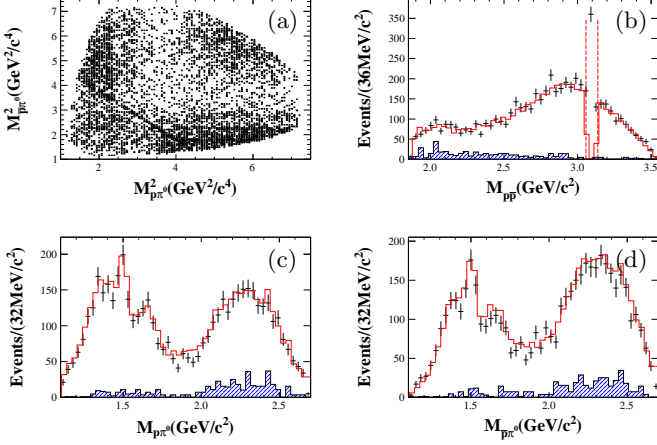


FIG. 1: (a) Dalitz plot of $\psi(3686) \rightarrow p\bar{p}\pi^0$, the invariant mass spectra of (b) $p\bar{p}$, (c) $p\pi^0$, and (d) $\bar{p}\pi^0$. The dashed lines in (b) show the cut at the J/ψ mass region. The crosses represent the experimental data, and the shaded histograms show the background from continuum process and π^0 sideband. The histograms in solid line show the sum of MC prediction and the background.

number of events, ξ is the four-momentum of p , \bar{p} and π^0 , $\omega(\xi)$ the probability density for a single event to populate the phase space at ξ , and $\epsilon(\xi)$ is the detection efficiency to detect one event with ξ . The free parameters c_i are determined by maximizing the likelihood function $\ln(L)$. For each N^* state, the amplitude is parameterized with a Breit-Wigner function, in which the mass and width of the resonance are variables, as described in [15]. The background contributions from π^0 sideband and continuum processes are removed by subtracting the log-likelihood ($\ln(L)$) values, as the log-likelihood value of data is the sum of that of signal and background events. Possible interference between continuum processes and $\psi(3686)$ decays is not considered.

All N^* resonances up to 2200 MeV/ c^2 with spin up to 5/2, listed in the summary tables of the Particle Data Book [21], are considered in this analysis, such as the well-established states, $N(1440)$ and $N(1520)$, and not-well-measured states, $N(2090)$ and $N(2100)$. Phase space decay and two speculative N^* resonances, $N(1885)$ and $N(2065)$ are also considered. According to the framework of soft π meson theory [22], the off-shell decay process is needed in this channel. Thus, $N(940)$ with a mass of 940 MeV/ c^2 and zero width is included. The $N(940)$ represents a virtual proton, which could emit a π^0 . The Feynman diagram of this process can be found in [15]. In total, nineteen intermediate resonances are considered.

For N^* resonances with spin larger than 5/2, such as the $N(2190)$, $N(2220)$, $N(2250)$ and $N(2600)$ [23–25], orbital angular momenta $L > 2$ are required, and are not expected to contribute significantly in charmonium decay

due to the suppression by the centrifugal barrier. The reason is two-fold. At first, the annihilation radius of $c\bar{c}$ is very small, estimated to be in the order of 0.1 fm, due to the large mass of charm quark. This is about one order of magnitude smaller than the interaction radius of πN scattering which is about several fm. Secondly, the relative momentum of N^* and \bar{p} is small, especially for large mass N^* resonance. Given the small annihilation radius and the small relative momenta of N^* and \bar{N} , orbital angular momenta $L > 2$ should be suppressed. If otherwise high spin states do exist in this decay, this should result in an inconsistency of data and fit, which is not observed. Thus, with the sensitivity of the present experiment, we consider it adequate to include only states with spin up to 5/2.

In our analysis, the first step is to select the significant resonances among all these resonances. The significance of each resonance is determined from the difference of the likelihood values of fits with and without the given resonance, accounting for the change of the number of parameters. Resonances with significance greater than 5σ are taken as significant ones and include $N(940)$ and seven N^* resonances. The remaining insignificant resonances are removed and only considered when estimating the systematic errors. The mass and width of N^* states are varied, and the values with the best fitting result are taken as the optimized values. Table I lists the optimized values for the seven N^* states. Here, the first errors are statistical and the second ones are systematic. In this table, the first five N^* resonances are consistent with the values in the Particle Data Book [21], while the last two states can not be identified with $N(2100)$ or $N(2200)$. However, the significance of these two states are 15σ and 11.7σ , respectively. As a consequence, we label these two states as $N(2300)$ and $N(2570)$, with J^P assignment of $1/2^+$ and $5/2^-$, respectively.

Using these eight significant resonances, the fit result agrees well with the data, as shown in Fig. 1. The χ^2 over the number of degree of freedom is 1.12. The contribution of each intermediate resonance including interference effects with other resonances are extracted and shown in Fig. 2. Plot (a) shows the contributions of $N(1440)$, $N(1520)$, $N(1535)$ and $N(1650)$ in which we can see clear peaks and also tails at the high mass region from the interference effects. Plot (b) shows the contributions of $N(940)$, $N(1720)$, $N(2300)$ and $N(2570)$. For $N(2300)$ and $N(2570)$, their peak positions are below the Breit-Wigner mean values reported in Table I because of the presence of interference contributions, as well as phase space and centrifugal barrier factors.

Various checks have been performed to test the reliability of this analysis. The first one is the spin parity check, in which the spin parity of each state of the optimized solution is changed to other possible values to test the other J^P assignments. For $N(2300)$ and $N(2570)$, $1/2^+$ and $5/2^-$, respectively, are the best

TABLE I: The optimized mass, width and significance (Sig.) of the seven significant N^* resonances. ΔS represents the change of the log likelihood value. ΔN_{dof} is the change of the number of free parameters in the fit. In the second and third columns, the first error is statistical and the second is systematic. The names of the last two resonances, $N(2100)$ and $N(2200)$, have been changed to $N(2300)$ and $N(2570)$ according to the optimized masses.

Resonance	$M(\text{MeV}/c^2)$	$\Gamma(\text{MeV}/c^2)$	ΔS	ΔN_{dof}	Sig.
$N(1440)$	1390^{+11+21}_{-21-30}	$340^{+46+70}_{-40-156}$	72.5	4	11.5σ
$N(1520)$	1510^{+3+11}_{-7-9}	115^{+20+0}_{-15-40}	19.8	6	5.0σ
$N(1535)$	1535^{+9+15}_{-8-22}	120^{+20+0}_{-20-42}	49.4	4	9.3σ
$N(1650)$	1650^{+5+11}_{-5-30}	150^{+21+14}_{-22-50}	82.1	4	12.2σ
$N(1720)$	1700^{+30+32}_{-28-35}	$450^{+109+149}_{-94-44}$	55.6	6	9.6σ
$N(2300)$	$2300^{+40+109}_{-30-0}$	$340^{+30+110}_{-30-58}$	120.7	4	15.0σ
$N(2570)$	2570^{+19+34}_{-10-10}	250^{+14+69}_{-24-21}	78.9	6	11.7σ

J^P values. The significance becomes worse using other J^P assignments. The second one is the Input-Output check. A MC sample was generated with given components. After the fitting procedure described above, the significant states and their properties (mass, width, branching fraction, and the effect of interference terms) are compared with the input values. The output values agree with the input within $\pm 1\sigma$, corroborating that the analysis procedure is reliable.

On the basis of the eight significant states, a scan for additional resonances has been performed with different spin parity, mass and width combinations. No extra resonance has been found to be significant. For $N(1885)$, the obtained significance ranges from 1σ to 1.2σ depending on the mass and width. The largest significance is obtained at a mass of $1930 \text{ MeV}/c^2$ and width of $150 \text{ MeV}/c^2$. The significance for $N(2065)$ varies between 3.2σ and 4σ , where the maximum is obtained at a mass of $2140 \text{ MeV}/c^2$ and width of $250 \text{ MeV}/c^2$. We consider neither resonance as significant and do not claim any evidence. Besides the known and speculative N^* resonances, a $1^{--} p\bar{p}$ resonance candidate described by the Breit-Wigner function has been added, as suggested by the near-threshold enhancement in the $p\bar{p}$ mass distribution. Varying the width from $50 \text{ MeV}/c^2$ to $300 \text{ MeV}/c^2$ and mass from $1800 \text{ MeV}/c^2$ to $3000 \text{ MeV}/c^2$ with the step size of $10 \text{ MeV}/c^2$, the largest significance obtained is 4σ at a mass of $2000 \text{ MeV}/c^2$ and width of $50 \text{ MeV}/c^2$, indicating that no $p\bar{p}$ resonance is required to explain the threshold enhancement.

The branching fraction of $\psi(3686) \rightarrow p\bar{p}\pi^0$ is determined as follows,

$$B(\psi(3686) \rightarrow p\bar{p}\pi^0) = \frac{N - N_{bkg}}{\epsilon \times N_{\psi(3686)} \times B(\pi^0 \rightarrow \gamma\gamma)}$$

$$= (1.65 \pm 0.03 \pm 0.15) \times 10^{-4}$$

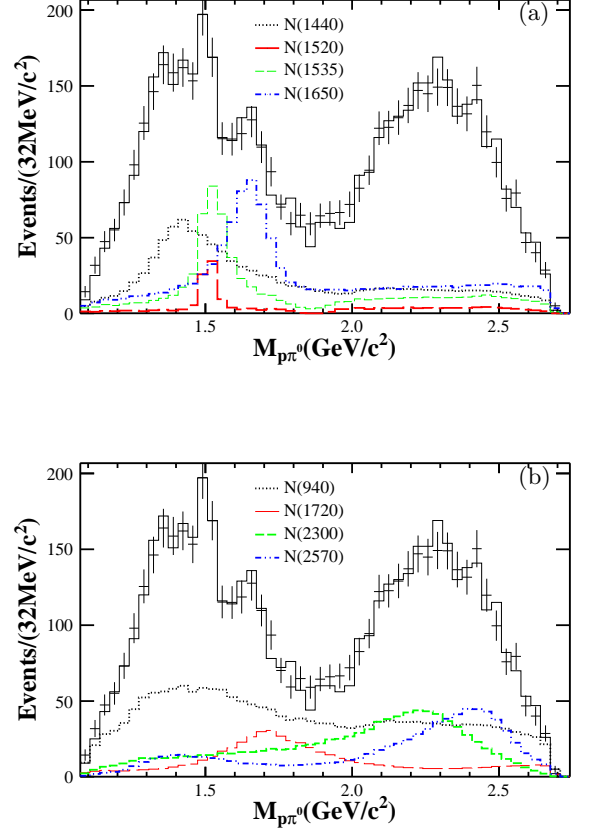


FIG. 2: The contribution of each intermediate resonance in the $p\pi^0$ mass spectra. The interferences with other resonances are included.

Here, N represents the number of observed events, N_{bkg} stands for the number of estimated background events, and ϵ is the efficiency derived from MC events generated according to the model derived from the PWA analysis. This result is in agreement with the value of $(1.33 \pm 0.17) \times 10^{-4}$ in the Particle Data Book [21]. The products of the production and decay branching fractions for each N^* intermediate resonance are also determined, as shown in Table II. The sum of the individual branching fractions is larger than the total due to interference effects of the intermediate resonances.

The systematic uncertainty sources are divided into two categories. The first includes the systematic errors from the number of $\psi(3686)$ events (4%), MDC tracking (4% for two charged tracks), particle identification (2% for both proton and anti-proton), photon detection efficiency (2%), and kinematic fit (7%). These uncertainties are applicable to all branching fraction measurements. The total systematic error from these common sources is 9.4%. The second source concerns the fitting procedure, which includes the uncertainties from

TABLE II: Summary of measurements of the number of events, the MC efficiency(ϵ), and the branching fraction (B.F.) of each intermediate resonance and the whole channel. Here, for the number of events and the branching fraction, the first error is statistical and the second is systematic.

Resonance	N	$\epsilon(\%)$	B.F.($\times 10^{-5}$)
$N(940)$	$1870^{+90+487}_{-90-327}$	27.5 ± 0.4	$6.42^{+0.20+1.78}_{-0.20-1.28}$
$N(1440)$	$1060^{+90+459}_{-90-227}$	27.9 ± 0.4	$3.58^{+0.25+1.59}_{-0.25-0.84}$
$N(1520)$	190^{+14+64}_{-14-48}	28.0 ± 0.4	$0.64^{+0.05+0.22}_{-0.05-0.17}$
$N(1535)$	$673^{+45+263}_{-45-256}$	25.8 ± 0.4	$2.47^{+0.28+0.99}_{-0.28-0.97}$
$N(1650)$	$1080^{+77+382}_{-77-467}$	27.2 ± 0.4	$3.76^{+0.28+1.37}_{-0.28-1.66}$
$N(1720)$	$510^{+27+50}_{-27-197}$	26.9 ± 0.4	$1.79^{+0.10+0.24}_{-0.10-0.71}$
$N(2300)$	$948^{+68+394}_{-68-213}$	34.2 ± 0.4	$2.62^{+0.28+1.12}_{-0.28-0.64}$
$N(2570)$	$795^{+45+127}_{-45-83}$	35.3 ± 0.4	$2.13^{+0.08+0.40}_{-0.08-0.30}$
Total	4515 ± 93	25.8 ± 0.4	$16.5 \pm 0.3 \pm 1.5$

additional possible resonances, the uncertainties using different Breit-Wigner parameterizations for partial wave amplitude, the uncertainties from background estimation, the uncertainties from the J/ψ exclusion cut, as well as the differences in the Input-Output check. These sources are applied to the mass, width and branching fraction measurements of intermediate states. The total systematic errors are the combination of the errors from the common sources and the fitting procedure.

In summary, we studied the intermediate resonances, including their masses, widths and spin parities, in the decay $\psi(3686) \rightarrow p\bar{p}\pi^0$. Two new N^* resonances are observed, in addition to five well-known N^* resonances. The masses and widths as well as the spin parities of the two new N^* states have been measured. The branching fractions of $\psi(3686) \rightarrow p\bar{p}\pi^0$ and the product branching fractions through each intermediate N^* state are measured. No clear evidence for $N(1885)$ or $N(2065)$ has been found. The hypothetical $p\bar{p}$ resonance has a significance of less than 4σ , indicating that the threshold enhancement most likely is due to interference of N^* intermediate resonances.

The BESIII collaboration thanks the staff of BEPCII and the computing center for their hard efforts. This work is supported in part by the Ministry of Science and Technology of China under Contract No. 2009CB825200; National Natural Science Foundation of China (NSFC) under Contracts Nos. 10625524, 10821063, 10825524, 10835001, 10935007, 11125525; Joint Funds of the National Natural Science Foundation of China under Contracts Nos. 11079008, 11179007; the Chinese Academy of Sciences (CAS) Large-Scale Scientific Facility Program; CAS under Contracts Nos. KJCX2-YW-N29, KJCX2-YW-N45;

100 Talents Program of CAS; Istituto Nazionale di Fisica Nucleare, Italy; U. S. Department of Energy under Contracts Nos. DE-FG02-04ER41291, DE-FG02-91ER40682, DE-FG02-94ER40823; U.S. National Science Foundation; University of Groningen (RuG); Helmholtzzentrum fuer Schwerionenforschung GmbH (GSI), Darmstadt; WCU Program of National Research Foundation of Korea under Contract No. R32-2008-000-10155-0.

-
- [1] S. Capstick and W. Roberts, Phys. Rev. D **47**, 1994 (1993).
 - [2] N. Isgur and G. Karl, Phys. Rev. D **19**, 2653 (1979).
 - [3] E. Santopinto, Phys.Rev.C **72**, 022201(R) (2005).
 - [4] M. Dugger *et al.* (CLAS Collaboration), Phys. Rev. C **76**, 025211 (2007).
 - [5] V. Kubarovsky *et al.* (CLAS Collaboration) Phys. Rev. Lett. **92**, 032001 (2004)
 - [6] S. Stepanyan *et al.* (CLAS Collaboration) Phys. Rev. Lett. **91**, 252001 (2003)
 - [7] M. Williams *et al.* (CLAS Collaboration) Phys. Rev. C **80**, 045213 (2009)
 - [8] M. Dugger *et al.* (CLAS Collaboration) Phys. Rev. Lett. **89**, 222002 (2002)
 - [9] I. Horn *et al.* (CB-ELSA Collaboration) Phys. Rev. Lett. **101**, 202002 (2008)
 - [10] O. Bartholomy *et al.* (CB-ELSA Collaboration) Phys. Rev. Lett. **94**, 012003 (2005)
 - [11] E. F. McNicoll *et al.* (Crystal Ball Collaboration at MAMI) Phys. Rev. C **82**, 035208 (2010)
 - [12] H. B. Li *et al.* (BES Collaboration), Nucl. Phys. A **675**, 189C (2000).
 - [13] J. Z. Bai *et al.* (BES Collaboration), Phys. Lett. B **510**, 75 (2001).
 - [14] M. Ablikim *et al.* (BES Collaboration), Phys. Rev. Lett. **97**, 062001 (2006).
 - [15] M. Ablikim *et al.* (BES Collaboration), Phys. Rev. D **80**, 052004 (2009).
 - [16] J. P. Alexander *et al.* (CLEO Collaboration), Phys. Rev. D **82**, 092002 (2010).
 - [17] M. Ablikim *et al.* (BES Collaboration), Nucl. Instrum. Meth. A **614**, 345 (2010).
 - [18] Rahul Sinha and Susumu Okubo, Phys. Rev. D. **30**, 2333-2344 (1984)
 - [19] W. Rarita, J. Schwinger, Phys. Rev. **60**, 61 (1941)
 - [20] W. H. Liang, P. N. Shen, J. X. Wang and B. S. Zou, J. Phys. G **28**, 333 (2002)
 - [21] C. Amsler *et al.*, Phys. Lett. B **667**, 1 (2008).
 - [22] L. Adler and R. F. Dashen, Current Algebra and Application to Particle Physics (Benjamin, New York, 1968); B. W. Lee, Chiral Dynamics (Gordon and Breach, New York, 1972).
 - [23] A. V. Anisovich *et al.*, Eur.Phys.J. A **48**(2012) 15
 - [24] R. A. Arndt *et al.*, Phys.Rev. C **74** (2006) 045205
 - [25] D. M. Manley *et al.*, Phys.Rev. D **45** (1992) 4002-4033